Supplemental Material for A physical interpretation of coupling chiral metaatoms

*Zhaolong Cao, Jianfa Chen, Shaozhi Deng, Huanjun Chen**

State Key Laboratory of Optoelectronic Materials and Technologies, Guangdong Province Key Laboratory of Display Material and Technology, School of Electronics and Information Technology, Sun Yat-sen University, Guangzhou 510275, China

Email: chenhj8@mail.sysu.edu.cn

Section S1. Symmetry requirement for chiral metasurface

Scattering matrix is a powerful tool for investigating the reflection and transmission properties of a photonic system. We start with the general S-matrix in the basis of linear polarizations. The input and output channels are defined in Fig. 1c in the main text. For plane waves traveling along the z-axis, the S-matrix formalism takes the form $|s_-\rangle = S|s_+\rangle$, or expressed explicitly by

$$\begin{pmatrix} s_{1-} \\ s_{2-} \\ s_{3-} \\ s_{4-} \end{pmatrix} = \begin{pmatrix} S_{11} & S_{12} & S_{13} & S_{14} \\ S_{12} & S_{22} & S_{23} & S_{24} \\ S_{13} & S_{23} & S_{33} & S_{34} \\ S_{14} & S_{24} & S_{34} & S_{44} \end{pmatrix} \begin{pmatrix} s_{1+} \\ s_{2+} \\ s_{3+} \\ s_{4+} \end{pmatrix}, \tag{S1}$$

where $s_{1+}(s_{3+})$ and $s_{2+}(s_{4+})$ are the x-polarized (y-polarized) light incident from $-z$ and $+z$ sides, and $s_{1-}(s_{3-})$ and $s_{2-}(s_{4-})$ are the x-polarized (y-polarized) light outgoing to $-z$ and $+z$ directions. Therefore, $|s_+\rangle = (1 \quad 0 \quad j \quad 0)^T/\sqrt{2}$ and $(0 \quad 1 \quad 0 \quad -j)^T/\sqrt{2}$ correspond to RCP incident light and $(1 \quad 0 \quad -j \quad 0)^T/\sqrt{2}$ and $(0 \quad 1 \quad 0 \quad j)^T/\sqrt{2}$ correspond to LCP incident light. The S-matrix is symmetric due to Lorentz reciprocity.

Next, we distinguish circular polarization conversion (CPC) and asymmetric transmission (AT) from 3D chirality. For circularly polarized light incident from the $-z$ side, the response of the system can be written as

$$|s_{R,-z}\rangle = \begin{pmatrix} S_{11} & S_{12} & S_{13} & S_{14} \\ S_{12} & S_{22} & S_{23} & S_{24} \\ S_{13} & S_{23} & S_{33} & S_{34} \\ S_{14} & S_{24} & S_{34} & S_{44} \end{pmatrix} \frac{1}{\sqrt{2}} \begin{pmatrix} 1 \\ 0 \\ i \\ 0 \end{pmatrix} = \frac{1}{\sqrt{2}} \begin{pmatrix} S_{11} + iS_{13} \\ S_{12} + iS_{23} \\ S_{13} + iS_{33} \\ S_{14} + iS_{34} \end{pmatrix}, \tag{S2.1}$$

$$|s_{L,-z}\rangle = \begin{pmatrix} S_{11} & S_{12} & S_{13} & S_{14} \\ S_{12} & S_{22} & S_{23} & S_{24} \\ S_{13} & S_{23} & S_{33} & S_{34} \\ S_{14} & S_{24} & S_{34} & S_{44} \end{pmatrix} \frac{1}{\sqrt{2}} \begin{pmatrix} 1 \\ 0 \\ -i \\ 0 \end{pmatrix} = \frac{1}{\sqrt{2}} \begin{pmatrix} S_{11} - iS_{13} \\ S_{12} - iS_{23} \\ S_{13} - iS_{33} \\ S_{14} - iS_{34} \end{pmatrix}, \tag{S2.2}$$

where $|s_{R,-z}\rangle$ and $|s_{L,-z}\rangle$ stand for RCP and LCP excitation from the $-z$ side. After some algebra operations, one obtains CD from $-z$ side

$$CD_{-z}=\frac{|t_+|^2-|t_-|^2}{|t_+|^2+|t_-|^2}=\frac{i\left(S_{12}^*S_{23}-S_{12}S_{23}^*+S_{14}^*S_{34}-S_{14}S_{34}^*\right)}{|S_{12}|^2+|S_{23}|^2+|S_{14}|^2+|S_{34}|^2}. \tag{S3.1}$$

Similarly, CD from $+z$ side can be calculated as

$$CD_{+z}=\frac{i\left(S_{12}S_{14}^*-S_{12}^*S_{14}+S_{23}S_{34}^*-S_{23}^*S_{34}\right)}{|S_{12}|^2+|S_{23}|^2+|S_{14}|^2+|S_{34}|^2}. \tag{S3.2}$$

To simplify Eq.S3, let us introduce

$$\beta_1=(S_{12}+S_{34})/2, \tag{S4.1}$$

$$\beta_2=(S_{12}-S_{34})/2, \tag{S4.2}$$

$$\gamma_1=(S_{14}+S_{23})/2, \tag{S4.3}$$

$$\gamma_2=(S_{14}-S_{23})/2. \tag{S4.4}$$

And $CD_{\pm z}$ can then be reduced to

$$CD_{\pm z}=\frac{2I\left(\beta_1^*\gamma_2\right)}{|\beta_1|^2+|\beta_2|^2+|\gamma_1|^2+|\gamma_2|^2}\pm\frac{2I\left(\beta_2\gamma_1^*\right)}{|\beta_1|^2+|\beta_2|^2+|\gamma_1|^2+|\gamma_2|^2}. \tag{S5}$$

Eq. S5 indicates that the CD signal has two origins. The first term in the right-handed side of Eq. S5 stays invariant when flipping illumination direction. This is exactly the definition of bi-isotropic(chiral) material,[1] and can be treated as 3D chirality. In contrast, the second term in the right-handed side of Eq. S5 flips its sign when changing illumination direction. This behavior is due to CPC and AT effects. To interpret this, we substitute Eq.4 into Eq.S2

$$|s_{R,-z}\rangle=\frac{1}{\sqrt{2}}\begin{pmatrix}S_{11}+iS_{13}\\S_{12}+iS_{23}\\S_{13}+iS_{33}\\S_{14}+iS_{34}\end{pmatrix}=\frac{1}{\sqrt{2}}\begin{pmatrix}S_{11}+iS_{13}\\0\\S_{13}+iS_{33}\\0\end{pmatrix}+\frac{\beta_1-i\gamma_2}{\sqrt{2}}\begin{pmatrix}0\\1\\0\\j\end{pmatrix}+\frac{\beta_2+i\gamma_1}{\sqrt{2}}\begin{pmatrix}0\\1\\0\\-j\end{pmatrix}, \tag{S6.1}$$

$$|s_{L,-z}\rangle=\frac{1}{\sqrt{2}}\begin{pmatrix}S_{11}-iS_{13}\\S_{12}-iS_{23}\\S_{13}-iS_{33}\\S_{14}-iS_{34}\end{pmatrix}=\frac{1}{\sqrt{2}}\begin{pmatrix}S_{11}-iS_{13}\\0\\S_{13}-iS_{33}\\0\end{pmatrix}+\frac{\beta_1+i\gamma_2}{\sqrt{2}}\begin{pmatrix}0\\1\\0\\-j\end{pmatrix}+\frac{\beta_2-i\gamma_1}{\sqrt{2}}\begin{pmatrix}0\\1\\0\\j\end{pmatrix}, \tag{S6.2}$$

Similarly, for the incidence from the $+z$ side

$$\left|s_{R,+z}\right\rangle = \frac{1}{\sqrt{2}}\begin{pmatrix} S_{12} - iS_{14} \\ S_{22} - iS_{24} \\ S_{23} - iS_{34} \\ S_{24} - iS_{44} \end{pmatrix} = \frac{1}{\sqrt{2}}\begin{pmatrix} 0 \\ S_{22} - iS_{24} \\ 0 \\ S_{24} - iS_{44} \end{pmatrix} + \frac{\beta_1 - i\gamma_2}{\sqrt{2}}\begin{pmatrix} 1 \\ 0 \\ -j \\ 0 \end{pmatrix} + \frac{\beta_2 - i\gamma_1}{\sqrt{2}}\begin{pmatrix} 1 \\ 0 \\ j \\ 0 \end{pmatrix}, \qquad \text{(S6.3)}$$

$$\left|s_{L,+z}\right\rangle = \frac{1}{\sqrt{2}}\begin{pmatrix} S_{12} + iS_{14} \\ S_{22} + iS_{24} \\ S_{23} + iS_{34} \\ S_{24} + iS_{44} \end{pmatrix} = \frac{1}{\sqrt{2}}\begin{pmatrix} 0 \\ S_{22} + iS_{24} \\ 0 \\ S_{24} + iS_{44} \end{pmatrix} + \frac{\beta_1 + i\gamma_2}{\sqrt{2}}\begin{pmatrix} 1 \\ 0 \\ j \\ 0 \end{pmatrix} + \frac{\beta_2 + i\gamma_1}{\sqrt{2}}\begin{pmatrix} 1 \\ 0 \\ -j \\ 0 \end{pmatrix}, \qquad \text{(S6.4)}$$

Obviously, the first term in the right-handed side of Eq.S6.1 – Eq.S6.4 corresponds to the reflection component, while the second term stands for the transmission component that preserves the handedness of incident light. For both incident conditions, this term only depends on the excitation handedness, and is invariant under different illumination directions. The third term in the right-handed side of Eq.S6 indicates the CPC. And importantly, it is also the cause of AT (e.g., under RCP excitation, the transmission difference between Eq. S6.1 and Eq. S6.3 also results from in the third term).

The above analysis indicates that, CPC and AT effects may cause nonzero CD signals. However, it is reported that they have no contribution to optical activity.[2-4] A convenient way to prevent CPC and AT effect is to impose C_4 rotational symmetry.[5, 6] That means the S-matrix is invariant with respect to a $\pi/2$ rotation about the z-axis. Using the coordinate transform matrix

$$T_{\pi/2} = \begin{pmatrix} & & -1 & \\ & & & -1 \\ 1 & & & \\ & 1 & & \end{pmatrix},$$

and solving the equation $S = T_{\pi/2}^{T} S T_{\pi/2}$, one obtains $\beta_2 = \gamma_1 = S_{13} = S_{24} = 0, S_{11} = S_{33}, S_{22} = S_{44}$. The S-matrix is then reduced to

$$S = \begin{pmatrix} S_{11} & \beta & & \gamma \\ \beta & S_{22} & -\gamma & \\ & -\gamma & S_{11} & \beta \\ \gamma & & \beta & S_{22} \end{pmatrix}. \qquad \text{(S7)}$$

Here the subscript of β and γ is dropped for simplicity.

In addition, reciprocal (Pasteur) bi-isotropic material also requires their reflection coefficient to be direction-independent, which means $S_{11} = S_{22}$. This condition is equivalent to the C_2 rotational symmetry along the x- or y-axis. Using the coordinate transform matrix to perform a π rotation about the y-axis

$$T_y = \begin{pmatrix} & -1 & & \\ -1 & & & \\ & & & 1 \\ & & 1 & \end{pmatrix}$$

and solving the equation $S = T_y^T S T_y$, one obtains $S_{11} = S_{22} = \alpha$.

When the metasurface both have out-of-plane (z-axis) C_4 and in-plane (x- and y-axis) C_2 rotational axes, it is equivalent to the D_4 symmetry. Therefore, a chiral metasurface analog to reciprocal (Pasteur) bi-isotropic material should have D_4 symmetry and the S-matrix takes the form

$$S = \begin{pmatrix} \alpha & \beta & & \gamma \\ \beta & \alpha & -\gamma & \\ & -\gamma & \alpha & \beta \\ \gamma & & \beta & \alpha \end{pmatrix}. \tag{S8}$$

Section S2. Derivation of background matrix C

Matrix C describes the background scattering when cavities are absent. Bounded by symmetry considerations, C will take the same form as Eq.S8. In addition, we assume the background medium is lossless, implying $C^{+} = C^{-1}$.[7] As a result, C can be derived as

$$C = e^{j\omega\delta} \begin{pmatrix} -\cos\xi & j\sin\xi\cos\chi & & j\sin\xi\sin\chi \\ j\sin\xi\cos\chi & -\cos\xi & -j\sin\xi\sin\chi & \\ & -j\sin\xi\sin\chi & -\cos\xi & j\sin\xi\cos\chi \\ j\sin\xi\sin\chi & & j\sin\xi\cos\chi & -\cos\xi \end{pmatrix}, \tag{S9}$$

where ξ and χ are arbitrary real parameters. We have deliberately dropped the universal phase factor δ through a particular choice of reference input plane.[7] In addition, a minus sign ($-$) is introduced in Eq. S9 following the standard convention. By assuming that the background chirality is negligible ($\chi = 0$), Eq. S9 reduces to Eq. 1 in the main text.

Section S3. Physical interpretation of matrix K

The excitation coefficient is defined as $K = (\kappa_1 \quad \kappa_2 \quad \cdots \quad \kappa_8)$ with κ_i being a 4×1 excitation vector for i^{th} cavity. According to time-reversal symmetry and conservation of energy, K should fulfill the following conditions[8]

$$CK^{*} = -K, \tag{S10.1}$$

$$K^{+}K = 2\Gamma, \tag{S10.2}$$

Note that solving Eq. S10.1 is equivalent to solve Eq. S11 for each κ_i vector

$$C\kappa_i^{*} = -\kappa_i. \tag{S11}$$

Together with the magnitude of κ_i: $|\kappa_i|^2/2 = \Gamma_{rad}$ representing the total radiative decay rate for i^{th} cavity, the general solution for Eq. S11 can be calculated as

$$\kappa_i = \sqrt{\Gamma_{rad}} \begin{pmatrix} & -j\sin\frac{\xi}{2}\sin\chi & \cos\frac{\xi}{2} & -j\sin\frac{\xi}{2}\cos\chi \\ j\sin\frac{\xi}{2}\sin\chi & & -j\sin\frac{\xi}{2}\cos\chi & \cos\frac{\xi}{2} \\ \cos\frac{\xi}{2} & -j\sin\frac{\xi}{2}\cos\chi & & j\sin\frac{\xi}{2}\sin\chi \\ -j\sin\frac{\xi}{2}\cos\chi & \cos\frac{\xi}{2} & -j\sin\frac{\xi}{2}\sin\chi & \end{pmatrix} X_i , \quad \text{(S12)}$$

where $X_i = \begin{pmatrix} x_{i1} & x_{i2} & x_{i3} & x_{i4} \end{pmatrix}^T$ is a dimensionless real vector with its magnitude $|X_i| = \sqrt{2}$. For negligible background chirality ($\chi = 0$), Eq. S12 yields

$$\kappa_i = \sqrt{\Gamma_{rad}} \begin{pmatrix} & & \cos\frac{\xi}{2} & -j\sin\frac{\xi}{2} \\ & & -j\sin\frac{\xi}{2} & \cos\frac{\xi}{2} \\ \cos\frac{\xi}{2} & -j\sin\frac{\xi}{2} & & \\ -j\sin\frac{\xi}{2} & \cos\frac{\xi}{2} & & \end{pmatrix} X_i . \quad \text{(S13)}$$

X_i is determined by the orientation of specific nanocavities. For example, considering the 1st nanorod that oriented along the x-axis (Fig. 1b), the longitudinal LSPR mode is given by $X_1 = \sqrt{2}\begin{pmatrix} 0 & 0 & \cos\phi & \sin\phi \end{pmatrix}^T$, where ϕ is a position parameter and will be discussed later. κ_i then can be conveniently expressed as

$$\kappa_1 = \sqrt{\Gamma_{rad}} \begin{pmatrix} \cos\frac{\xi}{2}x_{13} - j\sin\frac{\xi}{2}x_{14} \\ \cos\frac{\xi}{2}x_{14} - j\sin\frac{\xi}{2}x_{13} \\ \cos\frac{\xi}{2}x_{11} - j\sin\frac{\xi}{2}x_{12} \\ \cos\frac{\xi}{2}x_{12} - j\sin\frac{\xi}{2}x_{11} \end{pmatrix} = \sqrt{\Gamma_{rad}} \begin{pmatrix} \cos\frac{\xi}{2}\cos\phi - j\sin\frac{\xi}{2}\sin\phi \\ \cos\frac{\xi}{2}\sin\phi - j\sin\frac{\xi}{2}\cos\phi \\ 0 \\ 0 \end{pmatrix} . \quad \text{(S14)}$$

When nanorods are placed in a homogeneous environment, the background reflection is negligible ($\xi \sim \pi/2$) and κ_1 is then reduced to

$$\kappa_1 \sim \sqrt{\Gamma_{rad}} \begin{pmatrix} e^{-j\phi} \\ -je^{j\phi} \\ 0 \\ 0 \end{pmatrix} = \sqrt{\Gamma_{rad}} e^{-\frac{\pi}{4}j} \begin{pmatrix} e^{-j\left(\phi - \frac{\pi}{4}\right)} \\ e^{j\left(\phi - \frac{\pi}{4}\right)} \\ 0 \\ 0 \end{pmatrix} , \quad \text{(S15.1)}$$

As a result, the physical interpretation of ϕ is a retardation coefficient for $+z$ and $-z$ incoming waves, which is related to the layer distance and the wavevector of incoming waves by

$$kd = 2(\phi - \pi/4), \quad \text{(S15.2)}$$

or

$$\phi = kd/2 + \pi/4. \quad \text{(S15.3)}$$

Once the excitation vector for 1st nanorod is ready, the remaining nanocavities can be deduced from symmetry: $X_1 = - X_3 = \sqrt{2}(0 \quad 0 \quad \cos\phi \quad \sin\phi)^T$, $X_2 = - X_4 = \sqrt{2}(-\cos\phi \quad -\sin\phi \quad 0 \quad 0)^T$, $X_5 = - X_7 = \sqrt{2}(0 \quad 0 \quad -\sin\phi \quad -\cos\phi)^T$, $X_6 = - X_8 = \sqrt{2}(\sin\phi \quad \cos\phi \quad 0 \quad 0)^T$.

Section S4. The biorthogonal basis for matrix H

The biorthogonal product (also called c-product) is adopted from literature.[9, 10] In brief, let us denote the right (column) eigenvectors of H by v_i^R and the left (row) eigenvectors by v_i^L. We obtain

$$Hv_i^R = \omega_i v_i^R, \quad \text{(S16.1)}$$

$$v_i^L H = \omega_i v_i^L, \quad \text{(S16.2)}$$

where ω_i is the complex eigenfrequency of v_i^R and v_i^L. Given that H is a symmetric matrix, by taking the transpose of Eq. S16.2 one gets $H(v_i^L)^T = \omega_i (v_i^L)^T$, which means that the left and right eigenvectors for the same eigenfrequency are simply each other's transpose. Here, we consider the optical system without exceptional points. In this case, the eigenvectors form a complete set.[9] Next, let $X_R = (v_1^R \quad v_2^R \quad \cdots \quad v_n^R)$ be a matrix formed by the columns of the right eigenvectors and $X_L = X_R^T$ be a matrix formed by the rows of the left eigenvectors. Then

$$X_L H = H_0 X_L, \quad \text{(S17.1)}$$

$$HX_R = X_R H_0, \quad \text{(S17.2)}$$

where

$$H_0 = \begin{pmatrix} \omega_1 & \cdots & 0 \\ \vdots & \ddots & \vdots \\ 0 & \cdots & \omega_n \end{pmatrix}. \quad \text{(S17.3)}$$

By right-multiplying Eq. S17.1 with X_R and left-multiplying Eq. S17.2 with X_L, we have $X_L H X_R = H_0 X_L X_R = X_L X_R H_0$. Therefore, $X_L X_R$ must be a diagonal matrix. In the main text, the eigenvectors are normalized such that $X_L X_R \equiv 1$. Note that in this case $X_L^+ X_L \neq 1$, biorthogonal basis is no longer orthogonal in a conventional sense.

Section S5. Diagonalization of matrix H

Matrix H can be diagonalized via two steps. We start with the intralayer diagonalization from intralayer Hamiltonian first

$$X'_{L,intra} = X'_{R,intra} = \frac{1}{2}\begin{pmatrix} -1 & 1 & -1 & 1 \\ 1 & 1 & 1 & 1 \\ -1 & 1 & 1 & -1 \\ 1 & 1 & -1 & -1 \end{pmatrix}, \tag{S18.1}$$

$$X_{L1} = \begin{pmatrix} X'_{L,intra} & \\ & X'_{R,intra} \end{pmatrix} = X_{R1}, \tag{S18.2}$$

where $X'_{L,intra}$ is a matrix whose rows are the left eigenvectors of Ω_0 and $X'_{R,intra}$ is a matrix whose columns are the right eigenvectors of Ω_0. Left-multiply H by X_{L1} yields

$$X_{L1}H = H_1 X_{L1} = \begin{pmatrix} D_0 & S_{c1}^T \\ S_{c1} & D_0 \end{pmatrix} X_{L1}, \tag{S19.1}$$

where

$$D_0 = \begin{pmatrix} \tilde{\omega}_1 & & & \\ & \tilde{\omega}_2 & & \\ & & \tilde{\omega}_3 & \\ & & & \tilde{\omega}_3 \end{pmatrix}, \tag{S19.2}$$

$$S_{c1} = \begin{pmatrix} \tilde{\omega}_{15} & & & \\ & \tilde{\omega}_{26} & & \\ & & \tilde{\omega}_{37} & -\tilde{\omega}_{38} \\ & & \tilde{\omega}_{38} & \tilde{\omega}_{37} \end{pmatrix}, \tag{S19.3}$$

and $\tilde{\omega}_1$, $\tilde{\omega}_2$, $\tilde{\omega}_3$, $\tilde{\omega}_{15}$, $\tilde{\omega}_{26}$, $\tilde{\omega}_{37}$ and $\tilde{\omega}_{38}$ are given by

$$\tilde{\omega}_1 = \omega_0 - 2\omega_{12} - \omega_{13} + j\Gamma_{abs}, \tag{S19.4}$$

$$\tilde{\omega}_2 = \omega_0 + 2\omega_{12} - \omega_{13} + j\Gamma_{abs}, \tag{S19.5}$$

$$\tilde{\omega}_3 = \omega_0 + \omega_{13} + 2j\Gamma_{rad} + j\Gamma_{abs}, \tag{S19.6}$$

$$\tilde{\omega}_{15} = -\omega_{15} + \omega_{16} - \omega_{17} + \omega_{18}, \tag{S19.7}$$

$$\tilde{\omega}_{26} = -\omega_{15} - \omega_{16} - \omega_{17} - \omega_{18}, \tag{S19.8}$$

$$\tilde{\omega}_{37} = -\omega_{15} + \omega_{17} - 2j\Gamma_{rad}\sin 2\phi, \tag{S19.9}$$

$$\tilde{\omega}_{38} = \omega_{16} - \omega_{18}. \tag{S19.10}$$

Before performing the interlayer diagonalization, H_1 can be further reorganized by

$$T_1 = \begin{pmatrix} 1 & & & & & & & \\ & & & & 1 & & & \\ & 1 & & & & & & \\ & & & & & 1 & & \\ & & 1 & & & & & \\ & & & 1 & & & & \\ & & & & & & 1 & \\ & & & & & & & 1 \end{pmatrix}$$

for simplicity, yielding

$$H_2 = T_1 H_1 T_1^T = \begin{pmatrix} \tilde{\omega}_1 & \tilde{\omega}_{15} & & & & & & \\ \tilde{\omega}_{15} & \tilde{\omega}_1 & & & & & & \\ & & \tilde{\omega}_2 & \tilde{\omega}_{26} & & & & \\ & & \tilde{\omega}_{26} & \tilde{\omega}_2 & & & & \\ & & & & \tilde{\omega}_3 & & \tilde{\omega}_{37} & \tilde{\omega}_{38} \\ & & & & & \tilde{\omega}_3 & -\tilde{\omega}_{38} & \tilde{\omega}_{37} \\ & & & & \tilde{\omega}_{37} & -\tilde{\omega}_{38} & \tilde{\omega}_3 & \\ & & & & \tilde{\omega}_{38} & \tilde{\omega}_{37} & & \tilde{\omega}_3 \end{pmatrix}. \quad \text{(S20)}$$

Eq. S20 forms one of the central results of this work. That is, the mode hybridization of chiral metaatom can be divided into diagonal-block parts: $\begin{pmatrix} \tilde{\omega}_1 & \tilde{\omega}_{15} \\ \tilde{\omega}_{15} & \tilde{\omega}_1 \end{pmatrix}$, $\begin{pmatrix} \tilde{\omega}_2 & \tilde{\omega}_{26} \\ \tilde{\omega}_{26} & \tilde{\omega}_2 \end{pmatrix}$ and $\begin{pmatrix} \tilde{\omega}_3 & & \tilde{\omega}_{37} & \tilde{\omega}_{38} \\ & \tilde{\omega}_3 & -\tilde{\omega}_{38} & \tilde{\omega}_{37} \\ \tilde{\omega}_{37} & -\tilde{\omega}_{38} & \tilde{\omega}_3 & \\ \tilde{\omega}_{38} & \tilde{\omega}_{37} & & \tilde{\omega}_3 \end{pmatrix}$. A closer look at the eigenvectors of the intralayer eigenfrequency $\tilde{\omega}_1$ and $\tilde{\omega}_2$, one can find these eigenstates are dark modes - a direct consequence of the irreducible representations of the C_4 group (also a direct consequence of the circulant Ω_0 matrix).[5, 11] The dark modes can also be manifested by Eq. S19.4 and Eq. S19.5, where the imaginary parts of $\tilde{\omega}_1$ and $\tilde{\omega}_2$ only contain absorption terms. As a result, the radiative modes from H_3 contribute to chirality

$$H_3 = \begin{pmatrix} \tilde{\omega}_3 & & \tilde{\omega}_{37} & \tilde{\omega}_{38} \\ & \tilde{\omega}_3 & -\tilde{\omega}_{38} & \tilde{\omega}_{37} \\ \tilde{\omega}_{37} & -\tilde{\omega}_{38} & \tilde{\omega}_3 & \\ \tilde{\omega}_{38} & \tilde{\omega}_{37} & & \tilde{\omega}_3 \end{pmatrix}. \quad \text{(S21)}$$

We further perform interlayer diagonalization by

$$X_{L2} = X_{R2} = \frac{\sqrt{2}}{2} \begin{pmatrix} -1 & 1 & & & & & & \\ 1 & 1 & & & & & & \\ & & -1 & 1 & & & & \\ & & 1 & 1 & & & & \\ & & & & -1 & & \cos\zeta & \sin\zeta \\ & & & & & -1 & -\sin\zeta & \cos\zeta \\ & & & & \cos\zeta & -\sin\zeta & 1 & \\ & & & & \sin\zeta & \cos\zeta & & 1 \end{pmatrix}, \quad \text{(S22)}$$

where: $\sin\zeta = \dfrac{\tilde{\omega}_{38}}{\sqrt{\tilde{\omega}_{37}^2 + \tilde{\omega}_{38}^2}}$ and $\cos\zeta = \dfrac{\tilde{\omega}_{37}}{\sqrt{\tilde{\omega}_{37}^2 + \tilde{\omega}_{38}^2}}$. The H_0, $K^{'}$, $a^{'}$ and X_L defined in the main text are

$$H_0 = \begin{pmatrix} \tilde{\omega}_1 - \tilde{\omega}_{15} & & & & & & & \\ & \tilde{\omega}_1 + \tilde{\omega}_{15} & & & & & & \\ & & \tilde{\omega}_2 - \tilde{\omega}_{26} & & & & & \\ & & & \tilde{\omega}_2 + \tilde{\omega}_{26} & & & & \\ & & & & \tilde{\omega}_3 - \sqrt{\tilde{\omega}_{37}^2 + \tilde{\omega}_{38}^2} & & & \\ & & & & & \tilde{\omega}_3 - \sqrt{\tilde{\omega}_{37}^2 + \tilde{\omega}_{38}^2} & & \\ & & & & & & \tilde{\omega}_3 + \sqrt{\tilde{\omega}_{37}^2 + \tilde{\omega}_{38}^2} & \\ & & & & & & & \tilde{\omega}_3 + \sqrt{\tilde{\omega}_{37}^2 + \tilde{\omega}_{38}^2} \end{pmatrix}, \tag{S23.1}$$

$$K^{'} = KX_{R1}T_1^TX_{R2}, \tag{S23.2}$$

$$a^{'} = X_{L2}T_1X_{L1}a, \tag{S23.3}$$

$$X_L = X_{L2}T_1X_{L1} = X_R^T. \tag{S23.4}$$

Section S6. Derivation of $|s_-\rangle$

Considering that the first 4 eigenstates in Eq. S23.1 are dark modes. Eq. 5.1 and Eq. 5.2 in the main text can be further simplified by letting: $X_L = \begin{pmatrix} U_n & U_r \end{pmatrix}^T$, $K^{'} = \begin{pmatrix} 0 & K_r \end{pmatrix}$ and $H_r = diag(\omega_-, \omega_-, \omega_+, \omega_+)$, where U_n represents the dark modes, U_r is a 4×8 diagonalization matrix corresponding to chiral radiative modes, and $\omega_\pm = \tilde{\omega}_3 \pm \sqrt{\tilde{\omega}_{37}^2 + \tilde{\omega}_{38}^2}$. Therefore, the dynamic equations can be reduced to

$$\frac{d}{dt}(U_ra) = jH_r(U_ra) + K_r^T|s_+\rangle, \tag{S24.1}$$

$$|s_-\rangle = C|s_+\rangle + K_r(U_ra). \tag{S24.2}$$

Solving Eq. S24.1 and Eq. S24.2 yields the scattering matrix of the chiral system

$$|s_-\rangle = \left(C + K_r(j\omega I - jD_r)^{-1}K_r^T\right)|s_+\rangle = S|s_+\rangle. \tag{S25}$$

Given that $K_r = \begin{pmatrix} K_{r1} & K_{r2} & K_{r3} & K_{r4} \end{pmatrix}$, where K_{ri} is the excitation vector for i^{th} eigenstate. Eq. S25 can be simplified into

$$S = C + \frac{K_{r1}K_{r1}^T + K_{r2}K_{r2}^T}{j(\omega - \omega_-)} + \frac{K_{r3}K_{r3}^T + K_{r4}K_{r4}^T}{j(\omega - \omega_+)}, \tag{S26}$$

where

$$\frac{K_{r1}K_{r1}^T + K_{r2}K_{r2}^T}{j(\omega - \omega_-)} = \frac{2\Gamma_{rad}}{j(\omega - \omega_-)} \begin{pmatrix} \alpha_- & \beta_- & & \gamma_- \\ \beta_- & \alpha_- & -\gamma_- & \\ & -\gamma_- & \alpha_- & \beta_- \\ \gamma_- & & \beta_- & \alpha_- \end{pmatrix}, \tag{S27.1}$$

$$\frac{K_{r3}K_{r3}^T + K_{r4}K_{r4}^T}{j(\omega - \omega_+)} = \frac{2\Gamma_{rad}}{j(\omega - \omega_+)} \begin{pmatrix} \alpha_+ & \beta_+ & & \gamma_+ \\ \beta_+ & \alpha_+ & -\gamma_+ & \\ & -\gamma_+ & \alpha_+ & \beta_+ \\ \gamma_+ & & \beta_+ & \alpha_+ \end{pmatrix}, \tag{S27.2}$$

and

$$\alpha_{\pm} = \cos\xi(1 \mp \sin 2\phi \cos\zeta) - j\sin\xi(\sin 2\phi \mp \cos\zeta), \tag{S27.3}$$

$$\beta_{\pm} = \cos\xi(\sin 2\phi \mp \cos\zeta) - j\sin\xi(1 \mp \sin 2\phi \cos\zeta), \tag{S27.4}$$

$$\gamma_{\pm} = \mp \cos 2\phi \sin\zeta. \tag{S27.5}$$

To summarize, the scattering matrix can be expressed by

$$S = \begin{pmatrix} \alpha & \beta & & \gamma \\ \beta & \alpha & -\gamma & \\ & -\gamma & \alpha & \beta \\ \gamma & & \beta & \alpha \end{pmatrix}, \tag{S28.1}$$

$$\alpha = -\cos\xi + 4\Gamma_{rad}\frac{\cos\xi\left(\omega - \tilde{\omega}_3 - \sin 2\phi\tilde{\omega}_{37}\right) - j\sin\xi\left(\sin 2\phi\left(\omega - \tilde{\omega}_3\right) - \tilde{\omega}_{37}\right)}{j(\omega - \omega_-)(\omega - \omega_+)}, \tag{S28.2}$$

$$\beta = j\sin\xi + 4\Gamma_{rad}\frac{\cos\xi\left(\sin 2\phi\left(\omega - \tilde{\omega}_3\right) - \tilde{\omega}_{37}\right) - j\sin\xi\left(\omega - \tilde{\omega}_3 - \sin 2\phi\tilde{\omega}_{37}\right)}{j(\omega - \omega_-)(\omega - \omega_+)}, \tag{S28.3}$$

$$\gamma = \frac{-4\Gamma_{rad}\tilde{\omega}_{38}\cos 2\phi}{j(\omega - \omega_+)(\omega - \omega_-)}, \tag{S28.4}$$

where α is the reflection coefficient, and β and γ are transmission coefficients. As expected, the S-matrice in Eq. S27 and S28 take the form of Eq. S8, which prohibit the CPC and AT effects. This can be double-checked by examining the circularly polarized incidence

$$S\frac{1}{\sqrt{2}}\begin{pmatrix} 1 \\ 0 \\ \pm j \\ 0 \end{pmatrix} = \alpha\frac{1}{\sqrt{2}}\begin{pmatrix} 1 \\ 0 \\ \pm j \\ 0 \end{pmatrix} + (\beta \mp j\gamma)\frac{1}{\sqrt{2}}\begin{pmatrix} 0 \\ 1 \\ 0 \\ \pm j \end{pmatrix}, \tag{S29.1}$$

$$S\frac{1}{\sqrt{2}}\begin{pmatrix} 0 \\ 1 \\ 0 \\ \mp j \end{pmatrix} = \alpha\frac{1}{\sqrt{2}}\begin{pmatrix} 0 \\ 1 \\ 0 \\ \mp j \end{pmatrix} + (\beta \mp j\gamma)\frac{1}{\sqrt{2}}\begin{pmatrix} 1 \\ 0 \\ \mp j \\ 0 \end{pmatrix}. \tag{S29.2}$$

Section S7. Significance of doubly degenerate states

Generally speaking, for a 4-port cavity (R_1) that supports single resonant mode, and assuming its excitation coefficient is $\kappa_s = \begin{pmatrix}\kappa_{s1} & \kappa_{s2} & \kappa_{s3} & \kappa_{s4}\end{pmatrix}^T$, the scattering matrix can be written as[12]

$$S_1 = C_1 + \frac{\kappa_s \kappa_s^T}{j(\omega - \omega_1) + \Gamma_{tot1}}, \tag{S30.1}$$

$$\kappa_s \kappa_s^T = \begin{pmatrix} \kappa_{s1}^2 & \kappa_{s1}\kappa_{s2} & \kappa_{s1}\kappa_{s3} & \kappa_{s1}\kappa_{s4} \\ \kappa_{s1}\kappa_{s2} & \kappa_{s2}^2 & \kappa_{s2}\kappa_{s3} & \kappa_{s2}\kappa_{s4} \\ \kappa_{s1}\kappa_{s3} & \kappa_{s2}\kappa_{s3} & \kappa_{s3}^2 & \kappa_{s3}\kappa_{s4} \\ \kappa_{s1}\kappa_{s4} & \kappa_{s2}\kappa_{s4} & \kappa_{s3}\kappa_{s4} & \kappa_{s4}^2 \end{pmatrix}, \tag{S30.2}$$

where ω_1 is the (complex) resonant frequency, C_1 is the background scattering matrix and Γ_{tot1} is the total decay rate of R_1. Therefore, prohibited CPC and AT exists if and only if

$$\kappa_{s1}\kappa_{s3} = \kappa_{s2}\kappa_{s4} = 0, \tag{S31.1}$$

$$\kappa_{s1}\kappa_{s4} + \kappa_{s2}\kappa_{s3} = 0, \tag{S31.2}$$

$$\kappa_{s1}\kappa_{s2} - \kappa_{s3}\kappa_{s4} = 0, \tag{S31.3}$$

Apparently, there exist no nonzero solutions for Eq. S31, meaning that a single resonator can't support chiral modes analog to bi-isotropic materials.

In sharp contrast, considering another degenerate resonator (R_2) that possesses identical resonant frequency and total decay rate, whereas the excitation coefficient is rotated by $\pi/2$ about the z-axis ($\kappa_s^{'} = \begin{pmatrix}-\kappa_{s3} & -\kappa_{s4} & \kappa_{s1} & \kappa_{s2}\end{pmatrix}^T$)

$$S_1^{'} = C_1 + \frac{\kappa_s^{'} \kappa_s^{'T}}{j(\omega - \omega_1) + \Gamma_{tot1}}, \tag{S32.1}$$

$$\kappa_s^{'} \kappa_s^{'T} = \begin{pmatrix} \kappa_{s3}^2 & \kappa_{s3}\kappa_{s4} & -\kappa_{s1}\kappa_{s3} & -\kappa_{s2}\kappa_{s3} \\ \kappa_{s3}\kappa_{s4} & \kappa_{s4}^2 & -\kappa_{s1}\kappa_{s4} & -\kappa_{s2}\kappa_{s4} \\ -\kappa_{s1}\kappa_{s3} & -\kappa_{s1}\kappa_{s4} & \kappa_{s1}^2 & \kappa_{s1}\kappa_{s2} \\ -\kappa_{s2}\kappa_{s3} & -\kappa_{s2}\kappa_{s4} & \kappa_{s1}\kappa_{s2} & \kappa_{s2}^2 \end{pmatrix}. \tag{S32.2}$$

Once the R_1 and R_2 are present simultaneously, and note that for in-plane C_2 symmetry $\kappa_{s1}^2 + \kappa_{s3}^2 = \kappa_{s2}^2 + \kappa_{s4}^2$, the corresponding S-matrix are

$$S_1^{''} = C_1 + \frac{\kappa_s \kappa_s^T + \kappa_s^{'} \kappa_s^{'T}}{j(\omega - \omega_1) + \Gamma_{tot1}}, \tag{S33.1}$$

$$\kappa_s \kappa_s^T + \kappa_s^{'} \kappa_s^{'T} = \begin{pmatrix} \kappa_{s1}^2 + \kappa_{s3}^2 & \kappa_{s1}\kappa_{s2} + \kappa_{s3}\kappa_{s4} & & \kappa_{s1}\kappa_{s4} - \kappa_{s2}\kappa_{s3} \\ \kappa_{s1}\kappa_{s2} + \kappa_{s3}\kappa_{s4} & \kappa_{s2}^2 + \kappa_{s4}^2 & \kappa_{s2}\kappa_{s3} - \kappa_{s1}\kappa_{s4} & \\ & \kappa_{s2}\kappa_{s3} - \kappa_{s1}\kappa_{s4} & \kappa_{s1}^2 + \kappa_{s3}^2 & \kappa_{s1}\kappa_{s2} + \kappa_{s3}\kappa_{s4} \\ \kappa_{s1}\kappa_{s4} - \kappa_{s2}\kappa_{s3} & & \kappa_{s1}\kappa_{s2} + \kappa_{s3}\kappa_{s4} & \kappa_{s2}^2 + \kappa_{s4}^2 \end{pmatrix}, \qquad \text{(S33.2)}$$

which is the chiral formalism in Eq. S8 and S28.

Section S8. Full fitting results for numerically simulated metasurface

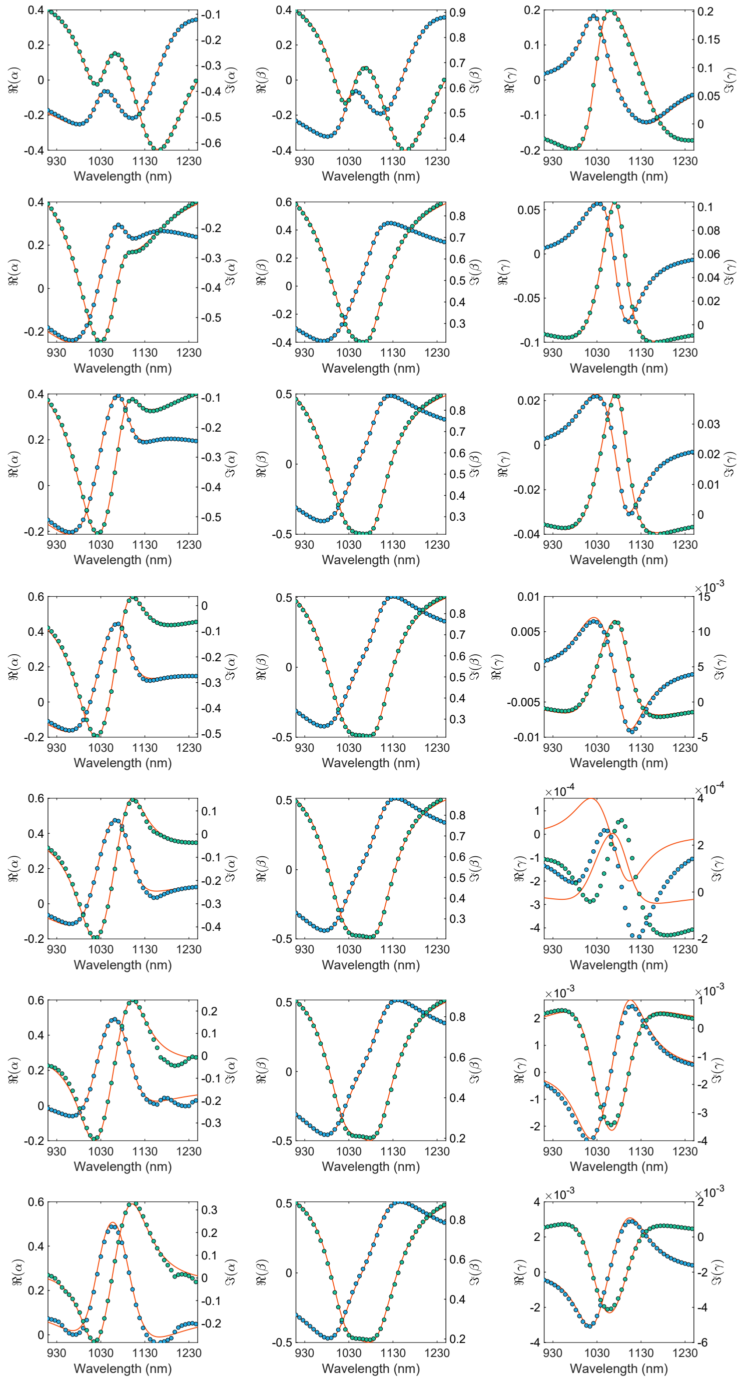

Fig. S1. Full fitting results for numerically simulated metasurface. Each rows from top to bottom correspond to $d =$ 40, 80, 100, 120, 140, 160, 180 nm. The fitting artifact for γ in $d = 140$ nm is attributed to the negligible chiral response of the metasurface.

Section S9. Evaluation of Γ_{abs} in CMT

We evaluate Γ_{abs} based on the $d = 60$ nm metasurface in the main text. First, we artificially reduce the Drude's damping rate of gold to 70%, 30%, and 0 of its original value. The simulated scattering coefficients are plotted in Fig. S2 as dotted lines. Next, we deduce the corresponding scattering coefficient based on fitted results from Fig 3d – 3f: $\omega_0 + \omega_{13} = 1.1679\ eV$, $-\omega_{15} + \omega_{17} = -7.6\ meV$, $\omega_{16} - \omega_{18} = 23.1\ meV$, $\Gamma_{rad} = 17.4\ meV$, $\Gamma_{abs} = 29.8\ meV$, $\phi = -2.08\ rad$, and $\xi = 1.62\ rad$. Γ_{abs} is proportionally reduced to $20.9\ meV$ (70%), $8.94\ meV$ (30%) and $0\ meV$. The CMT deduced scattering coefficients from Eq. S24 are plotted as the solid lines. As one can see, CMT predictions reconstruct the far-field property in excellent agreement, unambiguously confirming the applicability of chiral CMT.

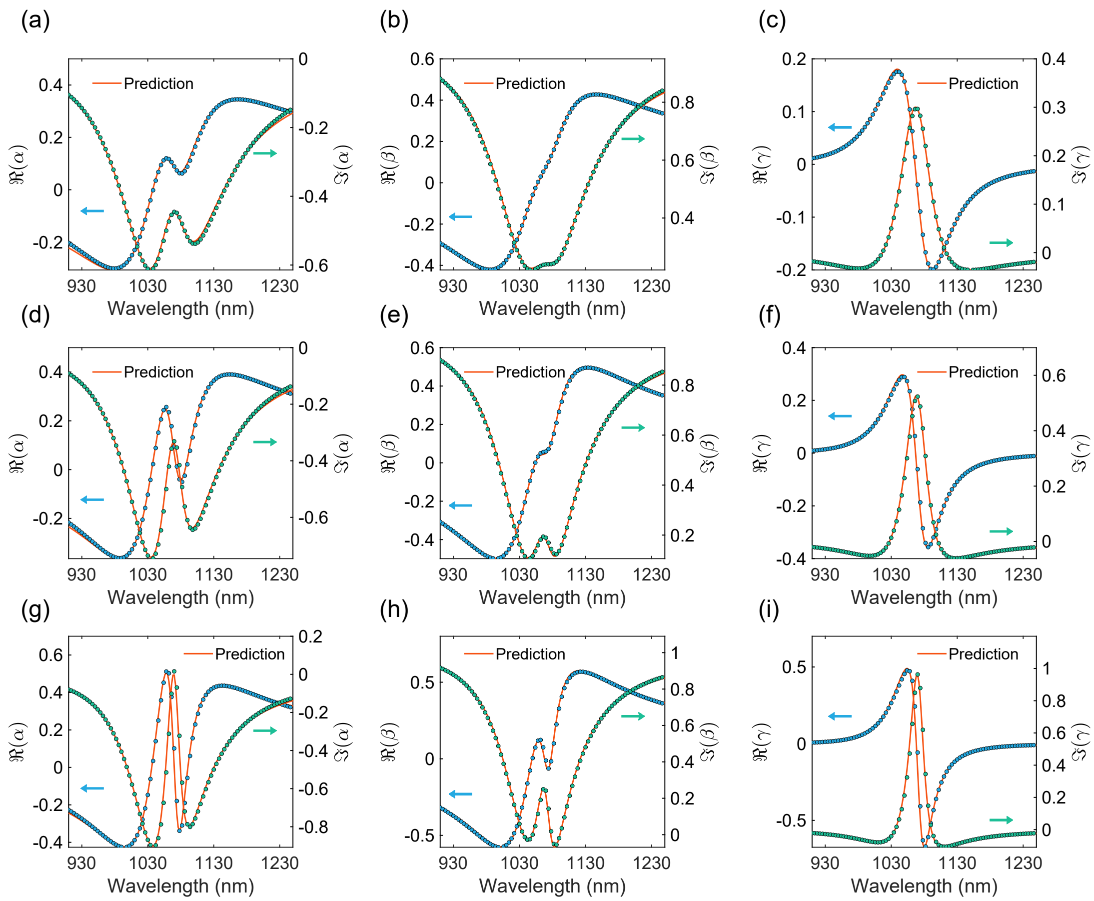

Fig. S2. Comparison between numerical simulations (dotted line) and CMT deduced (solid line) results. The scattering coefficient for 70% (a-c), 30% (d-f), and 0 (g-i) of gold's original Drude's damping rate are illustrated.

Reference:

1. I. V. Lindell, A. H. Sihvola, S. A. Tretyakov and A. J. Viitanen, *Electromagnetic Waves in Chiral and Bi-Isotropic Media*, Artech House, London, 1994.
2. J. Mun, M. Kim, Y. Yang, T. Badloe, J. Ni, Y. Chen, C.-W. Qiu and J. Rho, *Light Sci. Appl.*, 2020, **9**, 139.
3. O. Arteaga, J. Sancho-Parramon, S. Nichols, B. M. Maoz, A. Canillas, S. Bosch, G. Markovich and B. Kahr, *Opt. Express*, 2016, **24**, 2242-2252.
4. J. Sachs, J.-P. Günther, A. G. Mark and P. Fischer, *Nat. Commun.*, 2020, **11**, 4513.
5. M. V. Gorkunov, A. A. Antonov and Y. S. Kivshar, *Phys. Rev. Lett.*, 2020, **125**, 093903.
6. X. Yin, M. Schaferling, B. Metzger and H. Giessen, *Nano Lett.*, 2013, **13**, 6238-6243.
7. H. A. Haus, *Waves And Fields In Optoelectronics*, Prentice-Hall, Englewood Cliffs, N.J., 1984.
8. W. Suh, Z. Wang and S. H. Fan, *IEEE J. Quantum Electron.*, 2004, **40**, 1511-1518.
9. N. MOISEYEV, *Non-Hermitian Quantum Mechanics*, Cambridge University Press, 2011.
10. N. Moiseyev, P. R. Certain and F. Weinhold, *Mol. Phys.*, 1978, **36**, 1613-1630.
11. A. C. Overvig, S. C. Malek, M. J. Carter, S. Shrestha and N. Yu, *Phys. Rev. B*, 2020, **102**, 035434.
12. S. Fan, W. Suh and J. D. Joannopoulos, *J. Opt. Soc. Am. A*, 2003, **20**, 569-572.